DOE/ER/10107--3

DOE/ER-10107-3

DE82 003870

MICROSTRUCTURE OF RAPIDLY SOLIDIFIED Al_2O_3-DISPERSION-STRENGTHENED TYPE 316 STAINLESS STEEL

CONF-810831--18

J. Megusar, L. Arnberg, J.B. Vander Sande and N.J. Grant

Department of Materials Science and Engineering and Nuclear Reactor Laboratory
M.I.T., Cambridge, Massachusetts 02139, USA

An aluminum oxide dispersion strengthened 316 stainless steel was developed by surface oxidation. Surface oxidation was chosen as a preferred method in order to minimize formation of less stable chromium oxides. Ultra low C+N 316 stainless steel was alloyed with 1 wt% Al, rapidly solidified to produce fine powders and attrited to approximately 0.5 μm thick flakes to provide for surface oxidation. Oxide particles in the extruded material were identified mostly as Al oxides. In the preirradiated condition, oxide dispersion retarded crystallization and grain growth and had an effect on room temperature tensile properties. These structural modifications are expected to have an effect on the swelling resistance, structure stability and high temperature strength of austenitic stainless steels (Path A alloys).

1. INTRODUCTION

Austenitic stainless steels have been selected as prime candidate alloys in the Path A approach [1] and they show promise for early fusion power systems. The structure of Path A PCA alloys was controlled by rapid solidification (RS) [2]; a high density of heterogeneous nucleation sites for helium trapping was provided by reducing the grain size, by increasing the TiC particle/matrix interface area, and by introduction of high dislocation density. Irradiation experiments [3] indicate, however, that TiC coarsening may effectively limit the applications of TiC dispersion strengthened 316 stainless steel at higher irradiation temperatures. Consequently, we extended this research to prepare rapidly solidified, oxide dispersion strengthened type 316 stainless steel in order to study the effect of fine oxide particles on the high temperature strength, structure stability, and swelling resistance. It has been shown, based on a modeling approach [4] that Al_2O_3 should be more stable than TiC under irradiation conditions.

In the present study, the ultra low C+N 316 stainless steel was alloyed with 1 wt% Al, rapidly solidified to produce fine powders and attrited to fine flakes to provide for surface oxidation. The technique of surface oxidation has been explored as a preferred method of preparing OD alloys, based on a high Cr content.

2. EXPERIMENTAL PROCEDURES

The ultra low C+N 316 stainless steel was provided by Allegheny Ludlum Company and had the following chemical composition (in wt%): 16.36 Ni; 16.67 Cr; 2.26 Mo; 1.25 Mn; 0.51 Si; 0.0027 C; 0.003 N; 0.0027 S; bal. Fe. This alloy was remelted and modified by the addition of 1 percent aluminum. The amount and distribution of intermetallic phases were examined metallographically.

This material was rapidly solidified at Osprey Metals Ltd to produce fine powders by means of high velocity jets of nitrogen and argon. The estimated cooling rate was 10^4 K/sec. The powders were sieved into size fractions of -53; +53, -106; +106, -250 μm.

Powders finer than 53 μm were comminuted in an attritor mill using stainless steel balls; 200 g lots of powders were attrited under isopropyl alcohol for 17, 32 and 48 hrs at approximately 170 RPM. The accumulated flakes were decanted and vacuum dried. A quantity of 1100 g was cold compacted, degassed by heating to approximately 1000 K under vacuum and hot extruded at an area reduction ratio of 20:1 at 1420 K, resulting in a 1.1 cm diameter bar.

Rapidly solidified powders and attrited flakes were examined by scanning electron microscopy (SEM) and the surfaces of powders and attrited flakes were analyzed by scanning Auger microscopy (SAM). The microstructures of the consolidated material were examined by transmission electron microscopy (TEM) and scanning transmission electron microscopy (STEM). The STEM was equipped with an energy dispersive X-ray detector and an electron loss spectrometer. Samples were thinned by electropolishing in a 10% $HClO_4$-90%CH_3OH solution at 228 K and 25 V.

Microhardness testing was performed with a Tukon tester with a 200 g load. Room temperature tensile tests were performed on an Instron testing machine at a crosshead speed of 0.05 cm/min. Specimens were machined to ASTM specifications; test bars had a gage diameter of 0.406 cm and a gage length of 1.905 cm.

3. RESULTS AND DISCUSSION

3.1 Characterization of RS Powders

Figure 1 shows the morphology of rapidly

solidified powders with the size fraction below 38 μm. The microstructure of the powders which were metallographically polished and etched in glycerol regia is shown in Fig. 2; the dendrite arm spacing is typically 1-3 μm, indicating a cooling rate of approximately 10^{4} K/sec. Energy dispersive X-ray analysis obtained by Kevex EDXA (approximately 1 μm spatial resolution) failed to show segregation in the interdendritic areas, but Fig. 2 shows a fine dendritic structure.

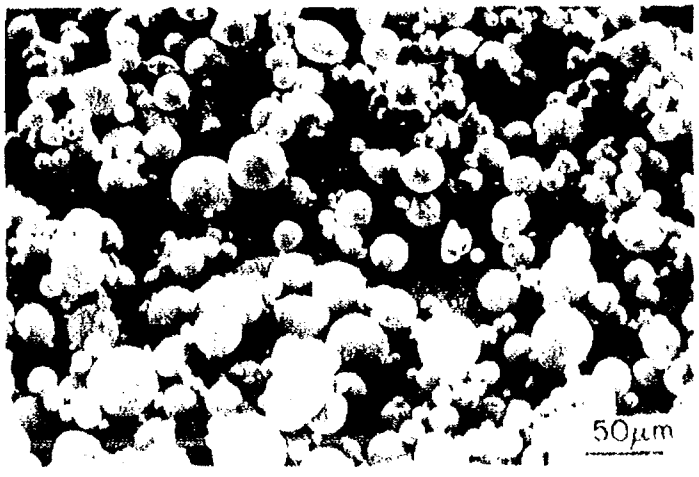

Fig. 1: SEM micrograph showing the morphology of rapidly solidified powders of 316 stainless steel alloyed with 1% Al. Size fraction below 38 μm.

Fig. 2: SEM micrograph showing the microstructure of rapidly solidified powders. Dendrite arm spacing is typically 1-3 μm.

Surfaces of rapidly solidified powders were analyzed by SAM. Concentration profiles for O, Al, Cr and Fe are shown in Fig. 3 and indicate an approximately 100 Å thick surface layer which is enriched in oxygen, aluminum and chromium.

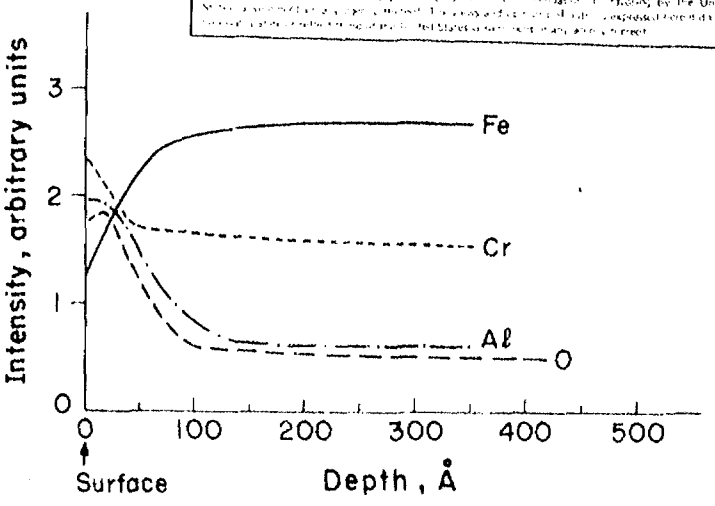

Fig. 3: Analysis of surfaces of rapidly solidified powders by SAM. Concentration profiles for O, Al, Cr and Fe are shown.

3.2 Characterization of Attrited Flakes

RS powders were attrited for 17, 32 and 48 hrs and the flake thickness and oxygen content were monitored as a function of attrition time in order to optimize conditions for surface oxidation. Results are summarized in Table 1 for a 48 h attrition time, which resulted in a uniform (0.25-0.50 μm) flake thickness and 0.42 wt% oxygen content. The morphology of the flakes after 48 h attrition is shown in Fig. 4.

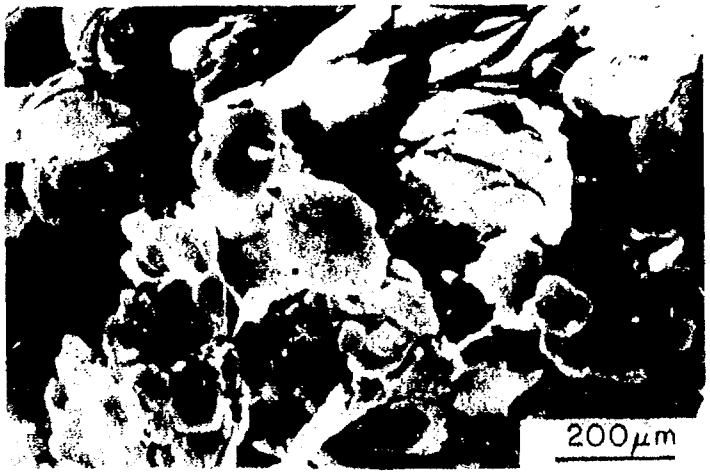

Fig. 4: SEM micrograph showing the morphology of attrited flakes. The 48 h attrition resulted in uniform (0.25-0.50 μm) flake thickness.

Concentration profiles for O, Al, Cr and Fe at the surface of the flakes (48 h attrition) are shown in Fig. 5 and indicate an approximately 100 Å thick surface layer enriched in O, Al and Cr, similar to that determined for the rapidly

Table 1: Variation of the flake thickness and oxygen content with attrition time.

Attrition time, h	Flake thickness μm	Oxygen Content wt%
16	0.5-3.5	n.d.
32	0.5-1.0	0.30
48	0.25-0.50	0.42

solidified powders (Fig. 3). Therefore, the attrition process of RS powders can be appropriately described as surface oxidation.

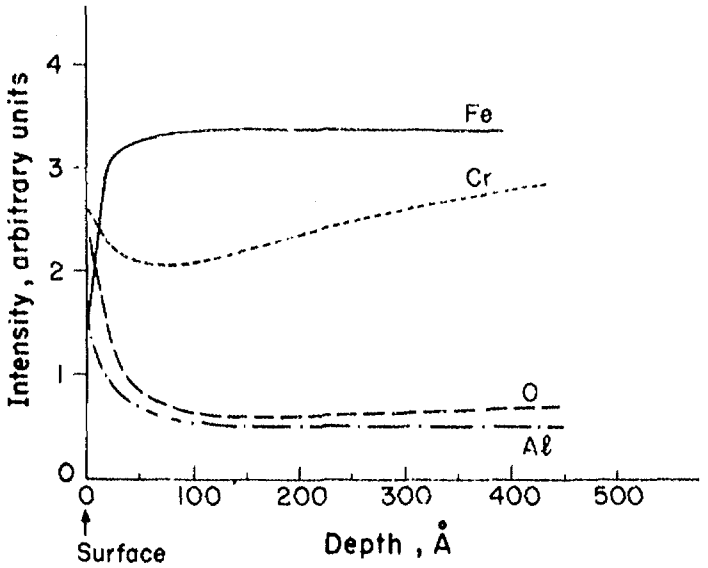

Fig. 5: Analysis of surfaces of attrited flakes by SAM. Concentration profiles for O, Al, Cr and Fe are shown.

3.3 Microstructure of the Extruded Material

The microstructure of the extruded material was examined by TEM. Extruded material was fully recrystallized, with an average grain size of 5 μm. The oxide layer which formed during powder attrition to produce flakes broke up during the extrusion process to form discrete oxide particles. They appear to be distributed randomly in the austenitic matrix.

Oxide size distribution and interparticle spacing were evaluated from TEM and SEM micrographs. The median oxide particle size is about 1000 Å and the average interparticle spacing is about 3000 Å. Particle number density, the interparticle spacing, and subsequent structural and mechanical properties of surface oxidized OD material can be varied, however, with the attrition conditions. As shown in Table 1, the flake thickness and oxygen content vary as a function of attrition time.

The composition of oxide particles was obtained by EDXA in a STEM. Most of the oxides can be identified as Al oxides, based on the energy dispersive X-ray spectrum, which showed a strong Al line (Fig. 6), and on the electron energy loss spectrum, showing an oxygen peak. No segregation was detected at the oxide particle/matrix interface.

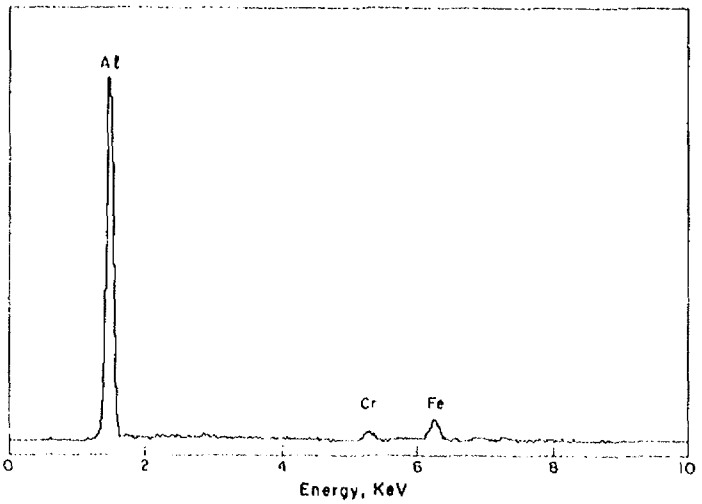

Fig. 6: Energy dispersive X-ray analysis (EDXA) of oxide particles in surface oxidized 316 stainless steel.

3.4 Microstructural Stability

The extruded material was subjected to different thermomechanical treatments (TMT's) in order to study microstructural stability. TMT's included cold swaging and annealing in the temperature range 873-1523 K. Knoop hardness was measured as a function of annealing temperature (1 h anneal). As shown in Fig. 7, hardness of the extruded material remained unchanged after 1 h anneal to 1423 K but dropped during annealing at 1523 K. TEM showed that the oxide dispersion effectively inhibited grain growth up to 1423 K annealing temperature; at 1523 K the grain size increased from 5 to 10 μm.

Knoop hardness increased from 225 (as-extruded condition) to 340 after cold swaging of the extruded material by 25 percent reduction of area. Subsequent annealing resulted in a gradual decrease in hardness until a fully annealed condition was reached at 1323 K (see Fig. 7). Hardness of the rapidly solidified and cold swaged Path A-1 alloy [5], on the other hand, decreased sharply in the temperature range 1023-1123 K when the fully annealed condition was obtained. The oxide dispersion therefore effectively stabilizes the microstructure of the RS austenitic stainless steel by retarding recrystallization and grain growth.

3.5 Microstructure of the Extruded and TMT Material

It was shown [6] that cold swaging plus intermediate annealing of oxide dispersed alloys sweeps many locations into low angle boundaries, permitting further cold work with less danger of cracking. Furthermore, intermediate annealing significantly modifies the dislocation density and distribution without greatly affecting the grain aspect ratio (GAR) and has therefore an important effect on the room temperature and high temperature mechanical properties [7].

Consequently, the extruded material was annealed 1 h at 1373 K and cold swaged to 25 percent reduction of area, with intermediate anneals (1 h at 973 K, see Fig. 7) after each 5-10 percent reduction of area. The microstructures are shown in Figs. 8 and 9. Fig. 8 shows the dislocation arrangements at the cell walls; cell sizes are typically 0.2-0.3 μm. Fig. 9 is a carbon extraction replica showing oxide particle distribution in the 25% CW material. Oxide particles largely reside in cell wall boundaries and effectively pin the cell walls.

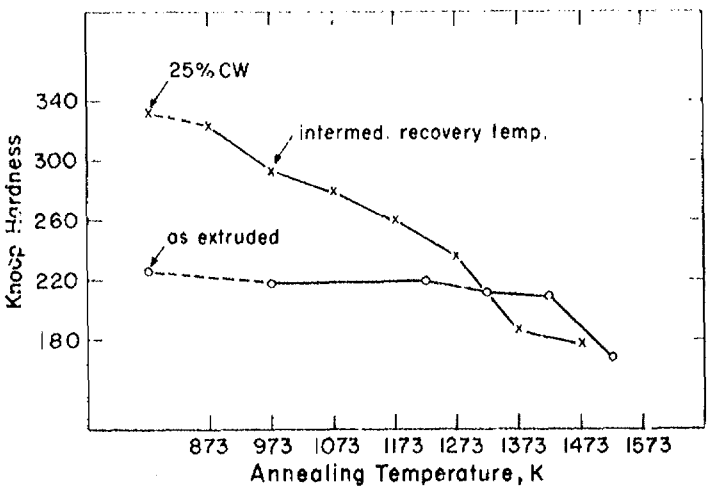

Fig. 7: Softening curves for the as-extruded RS 316 and 25% cold worked stainless steel. Plot of Knoop hardness versus annealing temperature (1 h anneal).

3.6 Room Temperature Tensile Properties

Room temperature tensile properties of OD stainless steel are shown in Table 2. The data for rapidly solidified Path A alloy are included for comparison.

The oxide dispersion increased the yield strength of the extruded material from 275 to 379 MPa while the ductility was reduced from 53.3 to 30.5%.

Fig. 8: TEM micrograph showing a microstructure of rapidly solidified and oxide dispersed 316 stainless steel in the 25% CW condition (transverse).

Fig. 9: Carbon extraction replica showing oxide particle distribution in rapidly solidified and oxide dispersed 316 stainless steel cold worked 25% (longitudinal).

Table 2: Room temperature tensile properties of Path A-1 and oxide dispersed 316 stainless steel.

ALLOY	Processing Condition	0.2%YS MPa	UTS MPa	Elong. %
Path A-1	Extruded	275	618	53.3
316, OD	Extruded	379	604	30.5
316, OD	Extruded+25%CW	750	759	10.3

CONCLUSIONS AND FUTURE WORK

A dispersion strengthened RS 316 stainless steel was developed by surface oxidation. Surface oxidation was chosen as a preferred method in order to minimize formation of less stable chromium

oxides. Ultra low C+N 316 stainless steel was alloyed with 1 %wt Al, rapidly solidified to produce fine powders and attrited to approximately 0.5 μm flakes to provide surface oxidation. Oxide particles in the extruded material were identified mostly as Al oxides.

In the preirradiated condition, oxide dispersion retarded crystallization and grain growth to very high temperature and improved room temperature tensile properties.

This research has been extended to study salt decomposition of refractory oxides on the attrited flakes as a means of supplying the desired oxide; alternatively, an oxide dispersed 316 stainless steel will be prepared by mechanical blending of fine refractory oxides with fine RS powders.

Irradiation testing (neutron and dual ion) is currently in progress to determine irradiation response of rapidly solidified and oxide dispersed 316 stainless steels.

ACKNOWLEDGEMENTS

This research has been supported by the U.S. Department of Energy, Office of Fusion Energy, under Contract No. DE-AC02-78ER-10107. Discussions with Professor O.K. Harling are gratefully acknowledged.

REFERENCES

[1] The Fusion Reactor Materials Program Plan; DOE/ET-0032/1.

[2] Megusar, J., Arnberg, L., Vander Sande, J.B., and Grant, N.J., this Conference.

[3] Maziasz, P.J., and Bloom, E.E., ADIP Quart. Prog. Rep., Jan-Mar 1978, p. 40; DOE/ET-0058/1.

[4] Frost, H.J., and Russell, K.C., Phase Stability Under Irradiation, DAFS Quart. Prog. Rep., May 1980, p. 133; DOE/ER-0046/1.

[5] Megusar, J., Arnberg, L., Vander Sande, J.B., and Grant, N.J., J. Nucl. Mater. (in press).

[6] Rasmussen, J.G., and Grant, N.J., Powder Met. 8 (1965) 92.

[7] Grewal, M.S., Sastri, S.A., and Grant, N.J., Metall. Trans. 6A (1975) 1393.

-END-

DATE FILMED

02/16/82